Monumental heritage exposure to urban black carbon pollution

D. Patrón[a], H. Lyamani[a,b], G. Titos[a,c], J.A. Casquero-Vera[a,b], C. Cardell[d], G. Močnik[e,f], L. Alados-Arboledas[a,b], F.J. Olmo[a,b]

[a]Andalusian Institute for Earth System Research, IISTA-CEAMA, University of Granada, Junta de Andalucía, Granada 18006, Spain

[b] Department of Applied Physics, University of Granada, Granada 18071, Spain

[c] Institute of Environmental Assessment and Water Research (IDÆA), Department of Geosciences, CSIC, Barcelona, Spain

[d] Dept. of Mineralogy and Petrology, Faculty of Science, University of Granada, Campus Fuentenueva s/n, Granada 18071, Spain

[e]Aerosol d.o.o. Research and Development Department, Ljubljana, Slovenia

[f]Department of Condensed Matter, Jozef Stefan Institute, Ljubljana, Slovenia

Correspondence to:

Lucas Alados Arboledas

Andalusian Institute for Earth System Research, IISTA-CEAMA, University of Granada, Junta de Andalucía, Granada 18006, Spain

email: alados@ugr.es

Abstract

In this study, aerosol light-absorption measurements obtained at three sites during a winter campaign were used to analyse and identify the major sources of Black Carbon (BC) particles in and around the Alhambra monument, a UNESCO World Heritage Site that receives over 2 million visitors per year. The Conditional Bivariate Probability Function and the Aethalometer model were employed to identify the main sources of BC particles and to estimate the contributions of biomass burning and fossil fuel emissions to the total Equivalent Black Carbon (EBC) concentrations over the monumental complex. Unexpected high levels of EBC were found at the Alhambra, comparable to those measured in relatively polluted European urban areas during winter. EBC concentrations above 3.0 $\mu g/m^3$, which are associated with unacceptable levels of soiling and negative public reactions, were observed at Alhambra monument on 13 days from 12 October 2015 to 29 February 2016, which can pose a risk to its long-term conservation and may cause negative social and economic impacts. It was found that road traffic emissions from the nearby urban area and access road to the Alhambra were the main sources of BC particles over the monument. However, biomass burning emissions were found to have very small impact on EBC concentrations at the Alhambra. The highest EBC concentrations were observed during an extended stagnant episode associated with persistent high-pressure systems, reflecting the large impact that can have these synoptic conditions on BC over the Alhambra.

Keywords: Black carbon aerosol, Aethalometers, stagnant atmospheric conditions, cultural heritage.

1. Introduction

Urban air pollution is a matter of great concern due to its adverse effects on human health and the environment. Although a number of European Directives and measures aimed at improving the air quality have been elaborated and implemented in recent years, concentrations of certain atmospheric pollutants continue exceeding legal limits and a large part of the European population are still exposed to high levels of these substances (EEA, 2016). In addition to the health and environmental adverse effects of air pollution, clear evidence exists on its negative impact on the historical heritage as well (e.g. Bonazza et al., 2007; Graue et al., 2013). In this context, the interest in better understanding the impacts of urban air pollution on cultural heritage has increased considerably (e.g. Nava et al., 2010; Ghedini et al., 2011; Krupińska et al., 2013). A large part of the historic-artistic heritage objects in cities are located in the open air, where different atmospheric processes and pollutants emitted mainly by road traffic, industry and domestic heating cause aesthetic and material damage (e.g. Horemans et al., 2011; Kontozova-Deutsch et al., 2011). These harmful effects may produce an irreversible deterioration of monuments and artworks over time and may also have significant economic and social impacts (e.g. Grossi and Brimblecombe, 2004; Fort, 2007; Urosevic et al., 2012). Therefore, the characterization and source identification of air pollutants in the vicinity of cultural heritage objects is necessary in order to provide sound scientific data and technical guidance that can help policy makers to develop more efficient preventive conservation measures and sustainable management (Ghedini et al., 2011; De la Fuente et al., 2013).

Ambient levels of sulphur dioxide (SO_2) in Europe have been drastically reduced over recent decades (Vestreng et al., 2007; Guerreiro et al., 2014) and consequently the adverse effects on historical heritage caused by this gaseous pollutant (e.g. corrosion and discoloration processes) have become less important (Ivaskova et al., 2015). However, concentrations of particulate matter (PM) have continued exceeding European air quality standards in urban and suburban areas (EEA, 2016). In the last years, several studies have focused on the relationship between this air pollutant and the gradual decay of historic monuments, paying special attention to the relevant role of carbonaceous particles, such as black carbon (BC), in black crust formation and other undesirable aesthetic effects (e.g. Rodríguez-Navarro and Sebastián, 1996; Sabbioni et al., 2003; Bonazza et al., 2005, 2007). In fact, BC is the principal agent in blackening the outdoor surfaces of heritage materials and Equivalent Black Carbon (EBC) concentrations above 2-3 $\mu g/m^3$ were found to be associated with unacceptable levels of soiling and negative public reactions (Brimblecombe and Grossi, 2005).

BC is the most strongly light-absorbing constituent of particulate matter in the atmosphere (Bond and Bergstrom, 2006; Moosmüller et al., 2009) with clear implications on the air quality (Querol et al., 2013). These particles are emitted directly from diesel engines (mainly from the traffic sector), open biomass burning and residential heating as a result of the incomplete combustion of carbonaceous fuels (e.g. Hamilton and Mansfield, 1991; Bond et al., 2004). Their mean atmospheric lifetime varies from a few days to weeks and they can be removed from the atmosphere via precipitation and dry deposition (Bond et al., 2013). BC is the dominant light-absorbing aerosol species in many European cities and represents a good primary tracer to assess the impact of vehicle traffic emissions on the environment (Reche et al., 2011).

The monumental complex of the Alhambra and Generalife (Granada, Spain) was a palatial citadel constructed from the 11th to the 15th century and represents a unique example of Islamic architecture in the Western world. One of the masterpieces of Nasrid art is the Patio de los Leones (Courtyard of the Lions), a rectangular courtyard surrounded by a low gallery supported on marble columns, which is located inside the palace complex. The famous Fountain of the Lions is situated at the middle of this courtyard and has recently been under restoration in an effort to preserve its integrity. The Alhambra was listed as UNESCO World Heritage Site in 1984 and is currently under intense pressure from tourism and urban development (over 2 million visitors in 2015 according to the Patronato de la Alhambra y Generalife). However, the influence of ambient air pollution, especially BC particles, on this artistic-historical monumental group has not been extensively studied (Horemans et al., 2011). The study of Horemans et al. (2011) focused on the analysis of indoor and outdoor atmospheric aerosol chemical composition (PM_1 and PM_{10-1}) and pollutant gases (O_3, NO_2, SO_2 and NH_3) measured at Alhambra and its surrounding during short summer (from 15th of June until 5th of July 2009) and winter campaigns (from 1st until 10th of February 2010). Although this last study pointed out to the traffic as one of the sources of particle matter and BC particles over Alhambra, detailed investigation of the sources of BC particles and their contributions to the total BC concentrations over the monumental complex was not previously done. Thus, the identification of the major sources of BC particles and the estimation of their contributions to the total EBC concentrations in and around the Alhambra monument can help us to provide information and operational guidance for a sustainable management by the competent authorities.

The intensity and duration of urban air pollution episodes not only depend on the amount of anthropogenic emissions but also on specific meteorological situations such as persistent high pressure system, low wind and, especially surface thermal inversion, which constrain horizontal and vertical dispersion of air pollutants (e.g. Charron and Harrison, 2003; Tiwari et al., 2013; Whiteman et al., 2014). In the urban area of Granada, located in a natural valley surrounded by high mountains (between 1000 and 3500 m a.s.l.), stagnant wintertime weather conditions associated with surface thermal inversions are relatively frequent and this contributes to a significant accumulation of fine anthropogenic particulate pollution near ground level (Lyamani et al., 2012). However, the influence of these stagnation episodes on BC concentrations at the Alhambra, located on the highest hill of the city, is unknown. Global climate change is expected to be accompanied by an increase in the frequency, duration and intensity of stagnation conditions, especially in Europe and North America (IPCC, 2013; Horton et al., 2014). Therefore, the analysis of BC particles during stagnation events will permit better understanding of the possible adverse effects of BC particles on monuments during future events.

Hence, the main aim of this study is the evaluation of the EBC concentrations and the identification of the major sources of BC particles as well as the estimation of their contributions to the total EBC concentrations in and around the Alhambra monument during winter. We also aim to investigate the impact of stagnant wintertime weather conditions on EBC concentrations in this monumental complex.

2. Methodology

2.1. Measurement sites

Equivalent black carbon measurements were performed at three different sites located in Granada city (37.16º N, 3.61º W, 680 m a.s.l.). Granada, situated in the south-eastern Iberian Peninsula, is a non-industrialized mid-size city with a population of 234 758 inhabitants, which increases up to 530 000 when including the metropolitan area (www.ine.es). The climate is typically Mediterranean-continental, with cool winters, dry and hot summers and large diurnal temperature variability. Due to its geographical position in the Mediterranean basin, Granada is influenced by two external aerosol source regions: Europe as a predominant source of anthropogenic pollution and North Africa as a principal source of natural dust (Alados-Arboledas et al., 2008; Lyamani et al., 2005, 2008). In the urban area of Granada, several authors have reported the importance of vehicle traffic emissions as a major local source of aerosol pollution (Titos et al., 2014), despite their relative decline during the economic crisis and the implementation of a new public transportation scheme in the last few years (e.g. Lyamani et al., 2008, 2010, 2011; Titos et al., 2015). Titos et al. (2014) found that road traffic exhaust emissions contribute around 50% to the fine fraction of particulate matter (PM_1; particles with aerodynamic diameter <1 μm) mass concentration during winter season. In this cold season, biomass burning from domestic heating and agricultural wastes burning represents an additional local source of BC particles in Granada urban area (Titos et al., 2017). The following lines briefly describe the three stations where the experimental measurements were performed (Fig. 1).

Fig. 1. Map of the city of Granada. The yellow triangles indicate the measurement stations.

- Patio de los Leones (PLE)

The famous “Patio de los Leones” or “Lion’s courtyard” (772 m a.s.l.) is the most visited jewel of Alhambra complex. This courtyard is an open site surrounded by a low gallery supported on marble columns. The famous Fountain of the Lions is situated at the middle of this courtyard and has recently been under restoration. The complete recovery of the original state of the Lion’s fountain took around 10 years and the courtyard was closed to visitors during part of the restoration process. Therefore, PLE is one of the Alhambra complex components with a high risk of suffering the effects of air pollution with important social and economic impacts. EBC measurements at this site started on 12 October 2015 and ended on 29 February 2016 (Table 1).

- La Mimbre (MIM)

La Mimbre or Casas de la Mimbre station (780 m a.s.l.) is located next to the main road traffic access to the Alhambra monument and public car park, on the Sabika hill. La Mimbre is around 500 m away from Patio de los Leones (PLE). EBC measurements at this location started on 18 November 2015 and ended on 17 December 2015 (Table 1).

- IISTA-CEAMA

The Andalusian Institute for Earth System Research (IISTA-CEAMA) is located in the southern part of the city (680 m a.s.l.). This station is included in EARLINET since 2004 (Pappalardo et al., 2014) and operates in the frame of ACTRIS observation network (http://actris.eu). The building is located in a pedestrian street near Camino de Ronda, one of the main arteries of Granada, and about 500 m from the busy A44 highway that surrounds the city (see Lyamani et al., 2008, 2010 for further details on the station). According to its location, the IISTA-CEAMA station can be considered as representative of urban background conditions. This site is 2 km away (straight line) from PLE and MIM stations. In this study we use measurements collected from 12 October 2015 till 29 February 2016 (Table 1).

Measurement station	Instrument	Measurement frequency	Period
IISTA-CEAMA	Aethalometer (Magee, AE33)	1 min	Oct 2015-Feb 2016
	Weather station	1 min	Oct 2015-Feb 2016
	Microwave radiometer (RPG-HATPRO)	1 min	Oct 2015-Feb 2016
PLE	Aethalometer (Magee, AE31)	5 min	Oct 2015-Feb 2016
MIM	Aethalometer (Magee, AE31)	5 min	Nov 2015-Dec 2015

Table 1: Measurement stations, instrumentation, frequency of sampling and measurement periods.

2.2. Measurements and instrumentation

2.2.1. Aethalometer measurements

In this work, two different models of Aethalometers (Magee Scientific Company, Berkeley, USA) were used to obtain EBC mass concentrations and multi-wavelength aerosol light-absorption coefficients at the three experimental sites: two units of model AE31 (Hansen et al., 1984) and one Aethalometer model AE33 (Drinovec et al., 2015). These instruments are based on filter technique and measure light attenuation (ATN) through a sample-laden filter at seven wavelengths: 370, 470, 520, 590, 660, 880 and 950 nm. According to the Lambert-Beer law, the attenuation is defined as:

$$\mathrm{ATN}(\lambda) = -100 \, . \ln\left(\frac{\mathrm{I}(\lambda)}{\mathrm{I}_0(\lambda)}\right) \qquad \textbf{(1)}$$

where I is the light intensity transmitted through the aerosol-loaded part of the filter tape and I_0 is the intensity of light passing through an original unloaded area of the filter. The attenuation coefficient (b_{ATN}) at each wavelength can be obtained by using the rate of ATN change with time (ΔATN/Δt) as follows:

$$\mathrm{b}_{\mathrm{ATN}} = \frac{1}{100} \; \frac{\mathrm{A} \; \Delta\mathrm{ATN}}{\mathrm{Q} \; \Delta\mathrm{t}} \qquad \textbf{(2)}$$

where A is the area of the sample spot and Q is the volumetric flow rate (set to 4 l min^{-1} in these instruments). This b_{ATN} can also be estimated from the EBC mass concentration reported by the Aethalometer as:

$$\mathrm{b}_{\mathrm{ATN}} = \mathrm{EBC} \; \sigma_{\mathrm{ATN}} \qquad \textbf{(3)}$$

where σ_{ATN} is the BC mass attenuation cross-section (provided by the manufacturer for the different wavelengths and Aethalometer models).

Following the recommendation proposed by ACTRIS (ACTRIS-2 WP3 Workshop, November 2015, Athens, Greece), a correction factor C_0 was applied to compensate the measurements, which are affected by different artefacts (e.g. Weingartner et al., 2003;

Virkkula et al., 2007). The absorption coefficients (σ_{ap}) at the seven wavelengths were calculated as shown in Eq. (4):

$$\sigma_{ap}(\lambda) = \frac{b_{ATN}(\lambda)}{C_0} \quad \textbf{(4)}$$

The recommended value of C_0 for Aethalometers AE31 is 3.5 assuming an uncertainty of ±25% and for the Aethalometer AE33, a value of 3.2 was used (ACTRIS-2 WP3 Workshop, November 2015, Athens, Greece).

The Absorption Ångström Exponent (AAE) was obtained from the linear fit based on Eq. (5), using hourly average values of σ_{ap} measured at 370, 520, 660 and 880 nm wavelengths:

$$\ln\left(\sigma_{ap}(\lambda_i)\right) = \ln\beta - \mathrm{AAE}\ln(\lambda_i) \quad \textbf{(5)}$$

This intensive parameter describes the spectral dependency of light absorption and it can also provide information about the predominant absorbing aerosol type and its origin (e.g. Cazorla et al., 2013; Valenzuela et al., 2015). AAE values ranging between 0.8 and 1.1 suggest the dominance of BC emitted by diesel engines while AAE values higher than 1.5 indicate considerable contribution from biomass burning (e.g. Kirchstetter et al., 2004; Bergstrom et al., 2002, 2007; Sandradewi et al., 2008). In this study, fits of the Ångström formula with R^2 lower than 0.85 were neglected in order to reduce noise.

Before starting the campaign, the Aethalometers were intercompared at the IISTA-CEAMA station for several days in order to assure the comparability of the measurements among the three experimental sites. The Aethalometer model AE33 participated in the ACTRIS inter-comparison (ACTRIS 2 Absorption Photometer Workshop, September 2015, Leipzig, Germany), which assures the high quality of the data used in this work. Therefore, this instrument was used as reference in this study. The factors obtained in the inter-comparison exercise allowed us to adjust the measurements of Aethalometers AE31 (PLE) and AE31 (MIM) to AE33. In addition, the Aethalometers data were processed in order to remove negative and extremely high values according to the criteria described by Segura et al. (2014).

2.2.2. Meteorological information

Meteorological variables, including ambient temperature, relative humidity, wind speed and rainfall, were measured by an automatic weather station at IISTA-CEAMA. Data collected as 1 min averages were processed to calculate hourly and daily means. Daily mean ambient temperature varied from 3 ºC to 19 ºC, with mean value of 12 ± 3 ºC during the analyzed period from 12 October 2015 to 29 February 2016. Daily mean relative humidity ranged between 36% and 80% with mean value of 60%. Both variables presented clear diurnal patterns with higher temperature and lower RH values at midday. The daily mean wind speed values ranged from 0.5 m s^{-1} to 4 m s^{-1}, showing a mean campaign value of 1.1 ± 0.5 m s^{-1}. There were 29 rainy days, with total accumulated rainfall of 134 l m^{-2} and maximum daily rainfall of 18 l m^{-1}.

Furthermore, a ground-based passive microwave radiometer (RPG-HATPRO, Radiometer Physics GmbH) operated at the IISTA-CEAMA station provided continuous temperature and humidity profiles from surface to 10 km during the studied period. The passive MWR performs zenith measurements of the sky brightness temperature with a radiometric resolution between 0.3 and 0.4 K root mean square error at 1s integration time (Navas-Guzmán et al., 2014). Temperature profiles are retrieved from surface temperature measurements and the brightness temperature measured at the V-band frequencies, where the first 3 frequencies (51.26, 52.28 and 53.86 GHz) are used only in zenith pointing and the last 4 (54.94, 56.66, 57.3 and 58 GHz) are considered for all the elevation angles (Meunier et al., 2013). A neural network algorithm (Rose et al., 2005) is used for retrieving temperature profiles with 0.8 K accuracy within the first 2 km, while 1.5 K accuracy is achieved between 2 and 4 km. The vertical resolution of the inversion varies with height, being 30 m on the ground, 50 m between 300-1200 m, 200 m between 1200 and 5000 m and 400 m above (Granados-Muñoz et al., 2012; Navas-Guzmán et al., 2014). Additional details of this instrument can be found in Granados-Muñoz et al. (2012) and Bravo-Aranda et al. (2017). In this work, an increase in temperature with height ($\Delta T/\Delta Z > 0$) was used to detect inversions near the surface and a thermal inversion episode was defined as a day with surface thermal inversion for at least 1 hour.

Synoptic pressure charts were obtained from the NOAA Air Resources Laboratory (http://ready.arl.noaa.gov/) to investigate the synoptic weather patterns that prevailed during the high BC concentration events classified as extreme episodes at the Alhambra monument. In this regard, “extreme BC” events have been defined as days in which the daily average EBC concentration at PLE attained or exceeded 3 μg/m^3; EBC concentrations associated with unacceptable levels of soiling and negative public reactions (Brimblecombe and Grossi, 2005). HYSPLIT4 (Hybrid Single Particle Lagrangian Integrated Trajectory, http://ready.arl.noaa.gov/HYSPLIT_traj.php) trajectories were analysed in order to determine the pathway and sources of the air masses that affected Granada during the extreme BC episodes. HYSPLIT4 model was used to compute 5-days air-mass back trajectories ending at 12:00 GMT at arrival altitudes of 500, 1000 and 1500 m a.g.l. over Granada. This model version uses the GDAS meteorological dataset (Global Data Assimilation System) with a spatial resolution of 1º x 1º and a temporal resolution of 3 hours (Stein et al., 2015; Rolph, 2017).

3. Results and discussion

3.1. Statistics of EBC mass concentrations and AAE

The distributions of daily averaged EBC mass concentration and AAE (370-880 nm) values for the period from 18 November to 17 December 2015, when the three stations operated simultaneously, are shown in Fig. 2. In order to investigate if there were statistical differences between EBC mass concentrations and AAE (370-880 nm) values observed at the three sites, we applied the Kolmogorov-Smirnov statistical test. According to this test, EBC concentrations registered at the three stations were significantly different at 95% confidence level. However, this test shows that the differences between AAE values obtained at the three sampling sites were not statically significant, indicating predominance of similar aerosol absorbing types. The mean EBC mass concentrations (± standard deviation) at PLE (2.3 ± 0.9 μg/m^3) and MIM (3.1 ± 1.1 μg/m^3) were significantly lower than at IISTA-CEAMA (4.9 ± 2.2 μg/m^3). This large difference between EBC mass concentrations measured in an urban background site within the city of Granada and the Alhambra area can be explained by the traffic restriction in the vicinity of the Alhambra monument. Also, part of this difference may be due to the location of the Alhambra monument on top of the Sabika hill, which is the highest point of the city, leading to relatively low pollution influence from Granada city. The lowest EBC mass concentrations were measured at PLE, located in the centre of the Alhambra complex and clearly separated from the direct impact of traffic. On the other hand, the mean values of AAE obtained at the three experimental stations during the period from November to December 2015 were similar (1.1 ± 0.2) and close to the expected value of 1 for fresh BC emitted by diesel engines (e.g. Bergstrom et al., 2002), suggesting that the main emission source of BC particles at the three sites is road traffic.

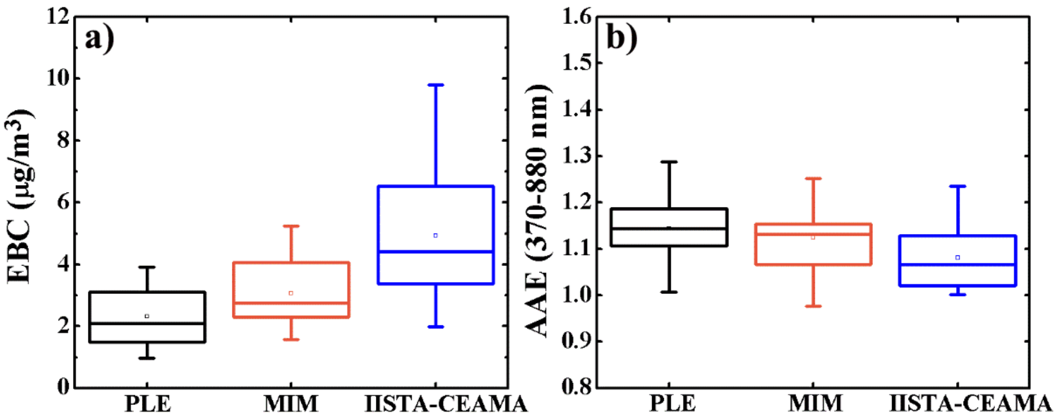

Fig. 2. Box and whisker plots of (a) EBC mass concentration and (b) AAE (370-880 nm) at the three measurements stations during the period from 18 November to 17 December 2015. The square marker inside the boxes represents the mean; the central line corresponds to the median; the box limits are the 25th and 75th percentiles and the whiskers correspond to 5th and 95th percentiles.

During the extended experimental campaign period from 12 October 2015 to 29 February 2016, when only PLE and IISTA-CEAMA stations operated simultaneously, the daily mean EBC mass concentrations at IISTA-CEAMA ranged from 0.6 to 10.3 μg/m^3 with mean value of 3.9 ± 2.0 μg/m^3. The EBC mass concentrations observed inside the Alhambra at PLE station were lower than those at IISTA-CEAMA and varied from 0.3 to 4.2 μg/m^3 with an average value of 1.8 ± 0.9 μg/m^3. The average EBC mass concentration at PLE was higher than the obtained by Horemans et al. (2011) in the Alhambra complex (1.0 μg/m^3) during summer 2009. This difference is mainly related to EBC seasonality. EBC concentrations at Granada city are higher in winter due the increase in emissions from domestic heating (e.g. Lyamani et al., 2011, 2012). Furthermore, EBC concentrations at PLE were in the upper range of values reported for other European urban areas (Table 2), increasing exposure of cultural heritage to BC pollution.

Location	Environment	Sapling period	Mean EBC (μg/m^3)	References
Seville, Spain	Urban	Winter 2013	1.56	Milford et al. (2016)
Huelva, Spain	Urban-Industrial	Winter 2013	0.71	Milford et al. (2016)
Barcelona, Spain	Urban	Winter 2004	2.60	Viana et al. (2007)
Toulon, France	Urban costal	Oct-Jan 2005	0.9	Saha and Despiau (2009)
Lugano, Switzerland	Urban-background	2009	1.8	Reche et al. (2011)
London, UK	Urban-background	2009	1.9	Reche et al. (2011)
Évora, Portugal	Urban	Winter 2007-2009	1.8	Pereira et al. (2012)

Table 2. EBC concentrations reported for other European urban areas.

3.2. Temporal variations of EBC mass concentrations and AAE

Hourly average values of EBC mass concentrations and AAE measured at PLE and MIM stations followed similar temporal evolutions from 18 November to 17 December 2015 due to the proximity between these locations (Fig. 3a). The hourly average values of EBC concentrations varied from 0.1 to 18.8 μg/m^3 inside the Alhambra palaces and from 0.1 to 19.2 μg/m^3 at MIM. The highest variability was observed at IISTA-CEAMA (0.1 to 28.6 μg/m^3) associated with its proximity to road traffic emissions. The sharp decrease in EBC concentration evident in all stations during 22-23 November was due to a rain episode. Higher EBC mass concentrations were observed at the three measurement sites from 1 to 17 December. The cause of these high levels is associated with a stagnation episode and will be examined in detail in the following sections. On the other hand, AAE showed a similar pattern at both PLE and MIM sites (Fig. 3b). Most of the hourly average values of AAE were within the range 0.8-1.2, indicating that in general BC particles over the three sites are originated from traffic emissions. However, hourly average values of AAE higher that 1.5 were also observed at the three sites, which may be associated with a significant contribution from biomass burning emissions.

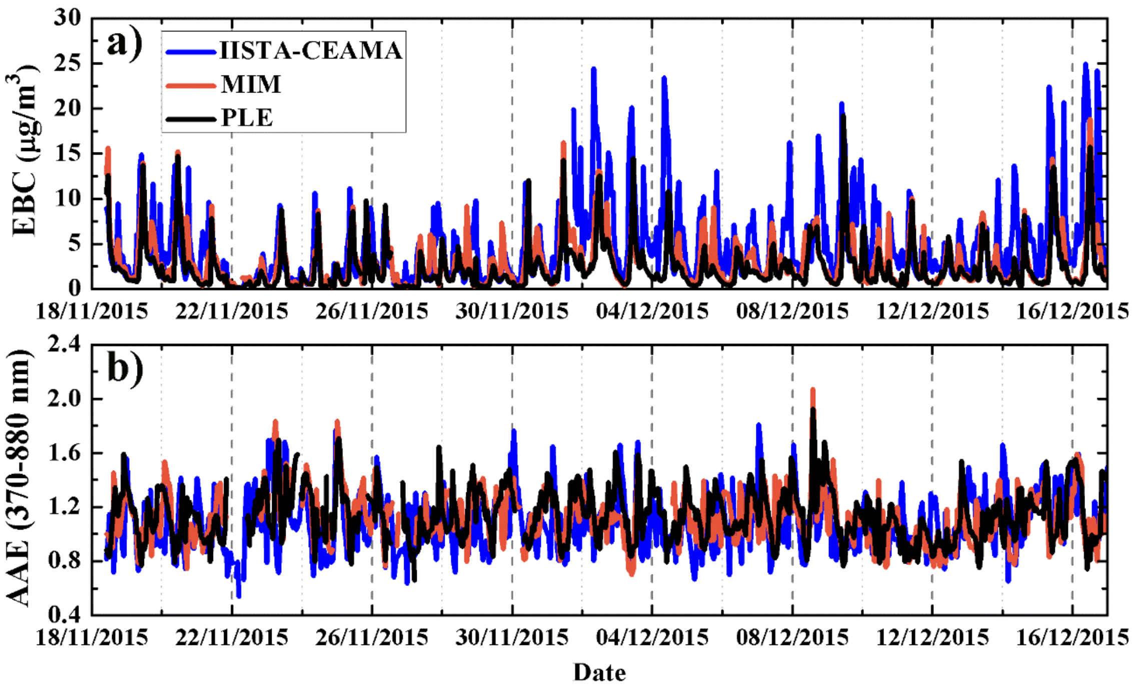

Fig. 3. Evolution of hourly mean values of (a) EBC mass concentration and (b) AAE (370-880 nm) at IISTA-CEAMA, MIM and PLE during the period from 18 November to 17 December 2015.

The upper panel of Fig. 4 shows the mean diurnal evolution of hourly EBC mass concentrations during workdays (Monday to Friday) and weekends (Saturday and Sunday) at PLE, MIM and IISTA-CEAMA. A clear diurnal cycle is observed at the three stations, especially marked at IISTA-CEAMA, with two maxima and two minima within a day. On workdays, the EBC concentration started to increase around 05:00 local time at IISTA-CEAMA, reaching a sharp peak in coincidence with traffic rush hours (around 09:00). The diurnal behaviour at PLE and MIM was very similar and the morning EBC peak was observed two hours later with respect to IISTA-CEAMA. This delay is likely due to the fact that the tourist traffic to access to the Alhambra monument starts slightly later than city traffic (mainly driven by working and school schedules). Another plausible explanation for this delay might be related to the daily evolution of planetary boundary layer (PBL) and surface winds. The diurnal minimum (between 15:00 and 16:00) can be explained by the relative decrease in traffic activities in combination with an increase in wind speed and PBL height that favour horizontal and vertical dispersion of BC particles (Lyamani et al., 2012). A second less pronounced peak was detected at the three sites during the evening traffic rush hours (around 18:00), being clearly visible at IISTA-CEAMA and MIM. The lowest diurnal EBC concentrations were observed after midnight, presumably due to a drastic decrease in traffic activities. On weekends, the morning EBC peaks were much lower compared to workdays. The mean EBC concentrations decreased between workdays and weekends by 2.2 $\mu g/m^3$ (67%) at IISTA-CEAMA, by 0.9 $\mu g/m^3$ (44%) at MIM and by 0.7 $\mu g/m^3$ (38%) at PLE, evidencing the large impact of traffic emissions on EBC mass concentrations over PLE and the other two sites. An interesting feature of Fig. 4 is that EBC concentrations at PLE and MIN stations were almost similar to the observed at IISTA-CEAMA between 11:00 and 16:00 local time. Plausible reason for this might be related to the daily evolution of planetary boundary layer and surface winds. Generally, between 11:00 and 16:00 local time both wind speed and PBL height reach its maximum favouring high horizontal and vertical dispersion of BC particles which lead to a more homogeneous distribution of black carbon particles over the studied area during this time of the day.

On the other hand, AAE presented the opposite diurnal pattern than EBC mass concentrations, with a well-defined minimum at PLE and two minima at IISTA-CEAMA and MIM (Fig. 4, lower panel). These diurnal cycles and minimum values (around 0.9 – 1) observed on workdays and weekends reinforce the idea that BC emissions from road traffic have a large influence on BC levels at the three sites. Relatively high AAE values were observed during the evening and night hours, which may be related to an increase in the relative contribution of biomass burning emissions from domestic heating and agricultural waste burning near Granada (Titos et al., 2017).

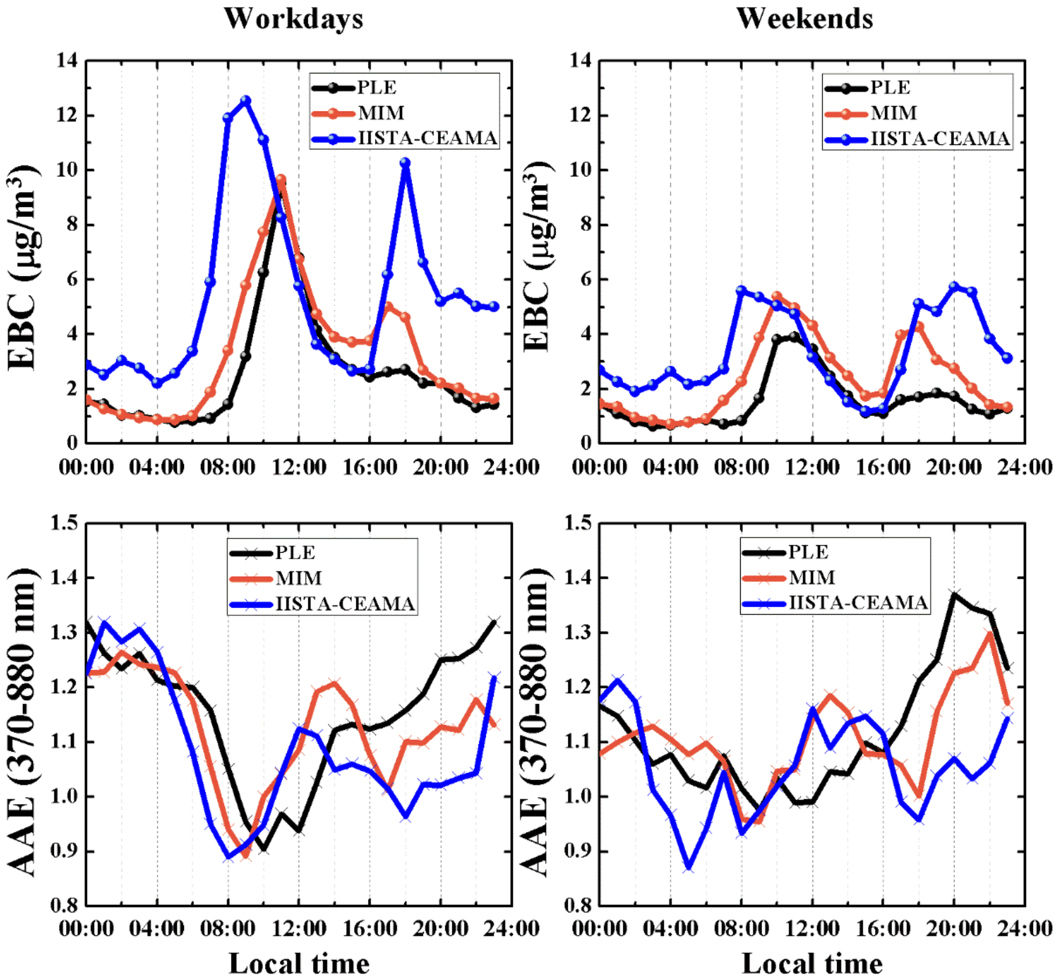

Fig. 4. Diurnal variation of hourly EBC mass concentration (upper panel) and AAE (370-880 nm) (lower panel) for workdays (Monday to Friday) and weekends (Saturday and Sunday) at PLE, MIM and IISTA-CEAMA.

3.3. Identification of BC source locations at the Alhambra monument

In order to identify the location of the main sources of BC particles over the Alhambra monument and its surroundings we have applied the Conditional Bivariate Probability Function, CBPF, method (Uria-Tellaetxe and Carslaw, 2014) to the 5-min EBC mass concentrations obtained at PLE station from 12 October 2015 to 29 February 2016. This technique is an extension of the Conditional Probability Function (CPF, Ashbaugh et al., 1985) and calculates the probability that the measured pollutant concentration exceeds a predetermined threshold value for a given wind sector with a particular wind speed, as shown in Eq. (6):

$$\mathrm{CBPF}_{\Delta\theta,\Delta u} = \frac{m_{\Delta\theta,\Delta u|EBC\geq X}}{n_{\Delta\theta,\Delta u}}$$

where $m_{\Delta\theta,\Delta u}$ is the number of samples in the wind sector $\Delta\theta$ with wind speed in the interval Δu having EBC concentrations higher than or equal to a threshold value x (concentrations >90th percentile, in this case) and $n_{\Delta\theta,\Delta u}$ is the total number of samples from the same wind direction-speed interval.

As can be seen in Fig. 5, the high EBC concentrations measured during the study period occurred with weak winds (<2 m/s) from the second and third quadrants (between 90 and 270 degrees), and particularly from southwest and southeast, corresponding to the directions where the city centre of Granada, the main road traffic access to the Alhambra and the A44 highway as well as the nearby agricultural lands are located (see Fig. 1). Therefore, this result indicates that the main sources of BC measured at the Alhambra monument and its surroundings are located in these sectors, where emissions from road traffic and biomass burning take place.

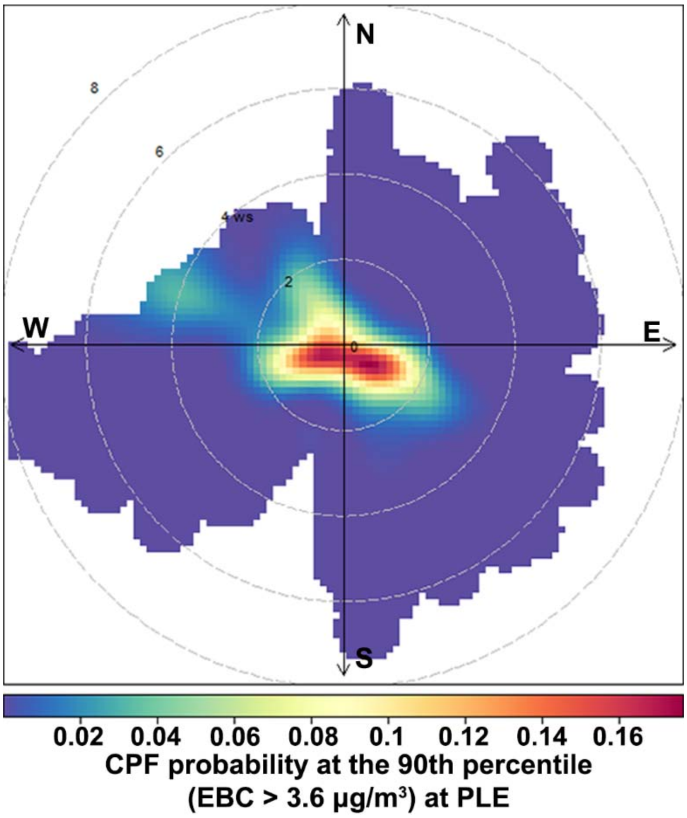

Fig. 5. CBPF plot of the EBC mass concentrations over PLE station for concentrations >90th percentile. The radial axis is wind speed in m/s. Plot is for 5-min data obtained from 12 October 2015 to 29 February 2016.

3.4. Quantification of biomass burning and traffic contributions to BC concentration at the Alhambra monument

During the autumn and winter months, the open burning of agricultural leftovers in the rural areas surrounding Granada is relatively frequent and, together with biomass burning from domestic heating, represents an additional source of BC particles during these seasons (Titos et al., 2017). The quantification of the contribution of these biomass emission sources to black carbon particles in close proximity to the Alhambra is important in order to design more effective measures for its preventive conservation. For this purpose, we have applied the Aethalometer model, a source apportionment method developed by Sandradewi et al. (2008) to estimate the carbonaceous material from fossil fuel (CM_{ff}) and biomass burning (CM_{bb}) employing the absorption coefficients (σ_{ap}) measured by a multi-wavelength Aethalometer. This model relies on the fact that the spectral absorption of the aerosol is composition-dependent, which is expressed through the AAE, and it assumes that road traffic and wood burning particles are the only ones that contribute to the total aerosol light absorption. Equivalent black carbon concentrations associated with traffic (BC_{ff}) and biomass burning (BC_{bb}) emissions can also be calculated with this method (e.g., Favez et al., 2010; Herich et al., 2011; Ealo et al., 2016). We have used hourly average values of σ_{ap} at 370 and 950 nm obtained at MIN, PLE and IISTA-CEAMA during the period from 18 November to 17 December 2015 and also the optimised source specific AAEs (AAE_{ff} = 0.9 and AAE_{bb} = 2.2 for this work) (Titos et al., 2017). At IISTA-CEAMA, an Aerosol Chemical Speciation Monitor (ACSM, Aerodyne Research Inc.) was operated during part of the campaign. The AAE values were optimized based on the best correlation between CM_{ff} and CM_{bb} with hydro-carbon like organic aerosols (HOA) and biomass burning organic aerosols (BBOA), respectively, obtained from the source apportionment of organic aerosol (Minguillón et al., 2015).

Fig. 6 shows the distributions of the estimated CM_{ff}, CM_{bb}, BC_{ff} and BC_{bb} concentrations for all stations during the period from 18 November to 17 December 2015, when the three Aethalometers operated simultaneously. The average contribution of fossil fuel emissions to CM at MIM and PLE was 57% (5.8 μg/m^3) and 56% (4.5 μg/m^3), respectively. The average contribution of biomass burning emissions was 43% (4.4 μg/m^3) at MIM and 44% (3.6 μg/m^3) at PLE. The CM_{ff} and CM_{bb} concentrations obtained at MIN and PLE stations were significantly lower than those obtained at IISTA-CEAMA (9.3 μg/m^3 for CM_{ff} and 6.8 μg/m^3 for CM_{bb}); although their relative contributions to CM were very similar (58% and 42%, respectively), indicating a homogeneous composition of CM in and around Granada. Similar results were obtained for IISTA-CEAMA and PLE for the period from 12 October 2015 to 29 February 2016.

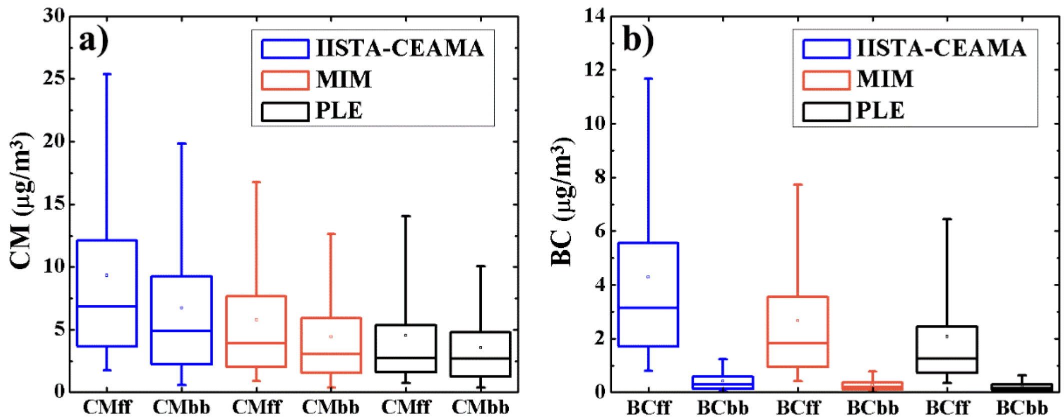

Fig. 6. Box plots of (a) CM_{ff} and CM_{bb} concentrations and (b) BC_{ff} and BC_{bb} at IISTA-CEAMA, MIN and PLE during the period from 18 November to 17 December 2015. The square marker inside the boxes represents the mean; the central line corresponds to the median; the box limits are the 25th and 75th percentiles and the whiskers correspond to 5th and 95th percentiles.

The CM_{ff} and CM_{bb} concentrations obtained at IISTA-CEAMA were very similar to those reported by Titos et al. (2017) for winter (November 2014 - February 2015) at IISTA-CEAMA (7.6 μg/m^3 for CM_{bb} and 8.5 μg/m^3 for CM_{ff}) and other urban site near the city centre of Granada (5.8 μg/m^3 for CM_{bb} and 8.1 μg/m^3 for CM_{ff}). Also, the relative contributions of fossil fuel and biomass burning emissions to total carbonaceous material at PLE, MIM and IISTA-CEAMA were very similar to those estimated by these authors (about 40% for CM_{bb} and 60% for CM_{ff}). These results show that both traffic and biomass burning emissions have a large impact on the CM levels observed at the study sites. However, the contribution of biomass burning source to EBC concentrations measured at the three stations was very small, as can be seen in Fig. 6b. In fact, the mean BC_{bb} contributions to the total EBC were 10% at MIN and PLE (0.3 μg/m^3 and 0.2 μg/m^3 respectively), and 9% (0.4 μg/m^3) at IISTA-CEAMA. The mean BC_{ff} concentrations were 2.7 μg/m^3 at MIM, 2.1 μg/m^3 at PLE and 4.3 μg/m^3 at IISTA-CEAMA. This information, together with the CBPF plot shown in Fig. 5, lead us to suggest that road traffic emissions from the southwest (city centre and A44 highway) and southeast (road traffic access to the monumental complex) parts of Granada urban area are the main sources of BC particles at the Alhambra monument.

3.5. Influence of meteorological conditions on extreme BC events

During the entire measurement period (from 12 October 2015 to 29 February 2016), we found 13 “extreme BC” days in which the daily average EBC concentration at PLE exceeded 3 μg/m^3; EBC concentrations associated with unacceptable levels of soiling and negative public reactions (Brimblecombe and Grossi, 2005). Table 3 lists the dates of these extreme BC events, average concentrations of EBC inside the Alhambra monument and mean wind speed. It can be noticed that all BC events occurred under low wind speed conditions (less than 1 m/s) being more frequent in December 2015. During this month, the surface synoptic situation was mainly dominated by persistent blocking high-pressure systems and weak pressure gradients over the Iberian Peninsula, with cloudless skies and lower minimum temperatures. These conditions promote the development of thermal inversions, which favour air stagnation and hence the accumulation of anthropogenic pollutants near the ground. Air mass back-trajectories calculated for each BC event confirm the anticyclonic curvature and the low speeds of the air masses arriving at Granada on these days. It seems clear, therefore, that extended stagnant meteorological conditions during synoptic high-pressure situations have a large influence on EBC concentrations with special repercussions at the Alhambra monument.

The most extreme episode recorded inside the Alhambra occurred on 2 December, as shown in Table 3. The synoptic conditions were very similar to those described above and the backward trajectories analysis indicated that the air masses came from North Africa through the southwestern Iberian Peninsula. However, there was no evidence of Saharan dust intrusion over the study area, according to the spectral analysis of the aerosol scattering and absorption coefficients (Valenzuela et al., 2015) and corroborated by MODIS images (not shown). The main difference between this event and the other extreme events was the development of a very shallow, strong and long-lasting thermal inversion at Granada on this day. As can be observed in Fig. 7, thermal inversion on 2 December was severe, with a base at the ground, top between 200 and 500 m a.g.l. and a positive temperature gradient of nearly 5 K/km in the early morning; ending around midday. This result reveals that the occurrence of strong surface thermal inversions at

Granada is a significant factor in the development and evolution of high BC concentration episodes at Alhambra monument.

Dates of events	EBC ($\mu g/m^3$)	Wind speed (m/s)
11/11/2015	3. ± 3.	0.8 ± 0.3
19/11/2015	3. ± 3.	0.7 ± 0.3
20/11/2015	3. ± 3.	0.8 ± 0.3
01/12/2015	3. ± 3.	0.7 ± 0.4
02/12/2015	4. ± 3.	0.6 ± 0.3
08/12/2015	3.1 ± 2.1	0.7 ± 0.3
09/12/2015	3. ± 4.	0.5 ± 0.2
15/12/2015	4. ± 4.	0.7 ± 0.3
16/12/2015	3. ± 4.	0.5 ± 0.2
14/01/2016	3. ± 4.	0.8 ± 0.4
22/01/2016	3.5 ± 2.8	0.8 ± 0.3
25/01/2016	3. ± 3.	0.7 ± 0.3
03/02/2016	3.1 ± 2.1	0.7 ± 0.4

Table 3: Daily averages of EBC concentration at PLE and daily mean wind speed during each extreme BC event identified during the period from October 2015 to February 2016.

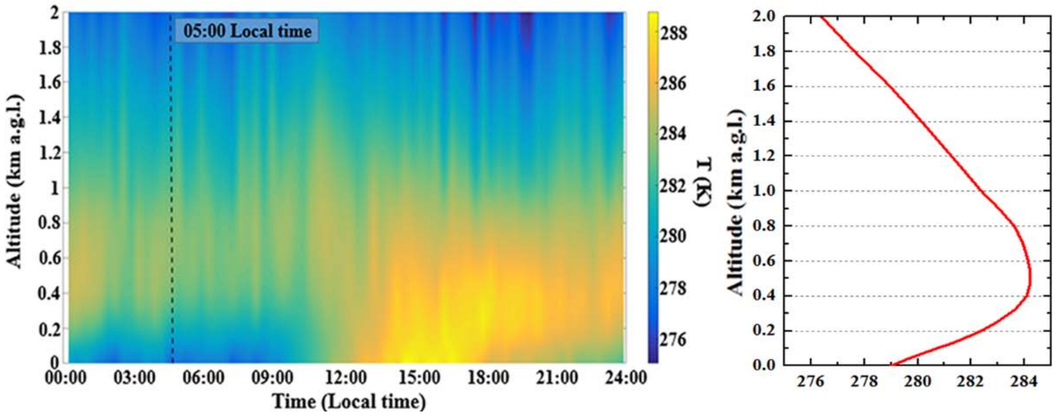

Fig. 7. Temporal variation of temperature profile (left panel) and temperature profile at 5:00 local time (right panel) up to 2 km a.g.l. at Granada during the intense stagnation episode (2 December 2015).

The analysis of the vertical temperature profiles measured by the passive microwave radiometer has allowed us to identify a total of 67 workdays with surface thermal inversions. This is about 80% of the workdays analysed during the entire measurement period (from 12 October 2015 to 29 February 2016), which reflects the persistence of stagnant conditions during the campaign. On the other hand, the strength, duration and depth of surface thermal inversions varied widely among these days.

The distributions of daily EBC mass concentrations for workdays with and without surface thermal inversion at PLE and IISTA-CEAMA stations are shown as box plots in Fig. 8. On workdays with surface inversions, the daily average EBC concentrations ranged from 0.8 to 4.2 μg/m^3 with an average value of 2.2 ± 0.8 μg/m^3 at PLE and varied from 1.4 to 10.3 μg/m^3 with mean value of 4.5 ± 1.7 μg/m^3 at IISTA-CEAMA. On workdays without surface thermal inversions, the daily EBC average concentrations varied from 0.5 to 1.5 μg/m^3 with mean value of 1.0 ± 0.4 μg/m^3 at PLE and ranged from 0.8 to 2.8 μg/m^3 with an average value of 1.9 ± 0.7 μg/m^3 at IISTA-CEAMA. Therefore, surface thermal inversion situations were associated with a 55 % increase in EBC mass concentration at PLE and a 58 % increase at IISTA-CEAMA. This large difference between inversion and non-inversion days highlights the large influence of meteorological conditions, and more specifically of surface thermal inversions, on BC concentrations at Alhambra monument.

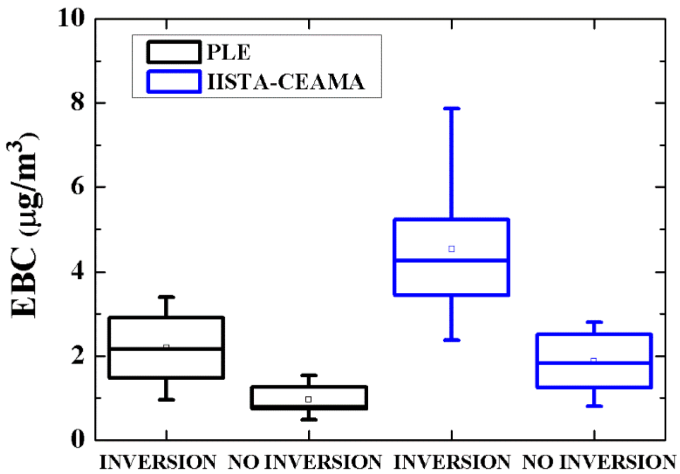

Fig. 8. Box plots of daily EBC mass concentrations for workdays with and without surface thermal inversions at PLE and IISTA-CEAMA. The squares are the mean values, the whiskers correspond to 5th and 95th percentiles, the box limits are the 25 and 75 percentiles and the mid line is the median.

4. Conclusions

EBC concentrations observed over the Alhambra monument and its surroundings were comparable to those measured in relatively polluted European urban areas during winter. Threshold EBC level (2-3 μg/m^3) suggested by Brimblecombe and Grossi (2005) as an acceptable EBC level for the exposure of buildings in urban areas, was exceeded at the Alhambra monument on 13 of the analyzed days in the period from 12

October 2015 to 29 February 2016. These situations may cause undesirable levels of soiling over time and, consequently, negative social and economic impacts.

The CBPF and Aethalometer model analyses revealed that road traffic emissions from the southwest (city centre and A44 highway) and southeast (road traffic access to the monumental complex) parts of Granada urban area were the main sources of BC particles over the Alhambra monument and its surrounding area. The results from the Aethalometer model also revealed that biomass burning emissions from the rural areas surrounding Granada have a large impact on carbonaceous material concentrations observed at the monumental complex during the analysed period. However, the contribution of biomass burning sources to EBC concentrations measured at the Alhambra monument and its surroundings was found to be very small; lower than 10%. This information can be very useful in order to improve the effectiveness of existing pollution abatement measures and also to formulate new strategies and measures aimed at reducing BC concentrations inside and around the monument.

The highest EBC concentrations measured at PLE and MIM occurred under stagnant weather conditions associated with surface thermal inversions during synoptic high-pressure situations, reflecting the large impact that these synoptic meteorological situations have on BC over the monumental complex. Stagnation events are expected to be more frequent and persistent in the future as consequence of continued global warming (Horton et al., 2014). Thus, this work features a case study where climate change can constitutes a major threat to cultural heritage, showing the significant effect of atmospheric conditions on atmospheric BC concentration at the Alhambra monumental complex, which can lead to increased surface blackening and may produce an irreversible deterioration.

Acknowledgments

This work was supported by the Andalusia Regional Government through project P12-RNM-2409 and P12-FQM-1889, by the Spanish Ministry of Economy and Competitiveness and FEDER through project CGL2013-45410-R, CGL2016-81092-R and CGL2012-30729, and by European Union's Horizon 2020 Research and Innovation Programme under grant agreement No. 654109, ACTRIS-2. The authors thank the Patronato de la Alhambra y Generalife for making this research possible.

References

ACTRIS 2, 2015. Absorption Photometer Workshop. http://actris-ecac.eu/files/AP-2015-1.pdf (last accessed April 2017).

Alados-Arboledas, L., Alcántara, A., Olmo, F.J., Martínez-Lozano, J.A., Estellés, V., Cachorro, V., Silva, A.M,. Horvath, H., Gangle, M. Días, A., Pujadas, M., Lorente, J., Labajo, A., Sorribas, M., Pavese G., 2008. Aerosol columnar properties retrieved from CIMEL radiometers during VELETA 2002. Atmos. Environ. 42 (11), 2654–2667.

Ashbaugh, L.L., Malm, W.C., Sadeh, W.Z., 1985. A residence time probability analysis of sulfur concentrations at Grand Canyon National Park. Atmos. Environ. 19 (8), 1263 –1270.

Bergstrom, R.W., Russell, P.B., Hignett, P., 2002. Wavelength dependence of the absorption of black carbon particles: predictions and results from the TARFOX experiment and implications for the aerosol single scattering albedo. J. Atmos. Sci. 59, 567 –577.

Bergstrom, R.W., Pilewskie, P., Russel, P.B., Redemann, J., Bond, T.C., Quinn, P.K., Sierau, B., 2007. Spectral absorption properties of atmospheric aerosols. Atmos. Chem. Phys. 7, 5937–5943.

Bonazza, A., Sabbioni, C., Ghedini, N., 2005. Quantitative data on carbon fractions in interpretation of black crusts and soiling on European built heritage. Atmos. Environ. 39 (14), 2607–2618.

Bonazza, A., Brimblecombe, P., Grossi, C.M., Sabbioni, C., 2007. Carbon in black crusts from the Tower of London. Environ. Sci. Technol. 41 (12), 4199–4204.

Bond, T. C., Streets, D. G., Yarber, K. F., Nelson, S.M., Woo, J.H., Klimont, Z., 2004. A technology-based global inventory of black and organic carbon emissions from combustion. J. Geophys. Res. 109 (D14), 203. http://dx.doi.org/10.1029/2003JD003697.

Bond, T.C., Bergstrom, R.W., 2006. Light absorption by carbonaceous particles: an investigative review. Aerosol Sci. Technol. 40 (1), 27–67.

Bond, T. C., Doherty, S. J., Fahey, D. W., Forster, P. M., Berntsen, T., DeAngelo, B. J., Flanner, M.G., Ghan, S., Kärcher, B., Koch, D., Kinne, S., Kondo, Y., Quinn, P.K., Sarofim, M.C., Schultz, M.G., Schulz, M., Venkataraman, C., Zhang, H., Zhang, S., Bellouin, N., Guttikunda, S.K., Hopke, P.K., Jacobson, M.Z., Kaiser, J.W., Klimont, Z., Lohmann, U., Schwarz, J.P., Shindell, D., Storelvmo, T., Warren, S.G., Zender, C.S., 2013. Bounding the role of black carbon in the climate system: A scientific assessment. J. Geophys. Res. Atmos., 118, no. 11, 5380-5552, doi:10.1002/jgrd.50171.

Bravo-Aranda, J. A., de Arruda Moreira, G., Navas-Guzmán, F., Granados-Muñoz, M. J., Guerrero-Rascado, J. L., Pozo-Vázquez, D., Arbizu-Barrena, C., Olmo Reyes, F. J., Mallet, M., Alados Arboledas, L., 2017. A new methodology for PBL height estimations based on lidar depolarization measurements: analysis and comparison against MWR and WRF model-based results. Atmos. Chem. Phys., 17, 6839-6851. https://doi.org/10.5194/acp-17-6839-2017.

Brimblecombe, P., Grossi, C.M., 2005. Aesthetic thresholds and blackening of stone buildings. Sci. Total Environ. 349 (1), 175–189.

Cazorla, A., Bahadur, R., Suski, K.J., Cahill, J.F., Chand, D., Schmid, B., Ramanathan, V., and Prather, K. A,. 2013. Relating aerosol absorption due to soot, organic carbon, and dust to emission sources determined from in-situ chemical measurements. Atmos. Chem. Phys. 13, 634 9337–9350.

Charron, A., Harrison, R.M., 2003. Primary particle formation from vehicle emissions during exhaust dilution in the roadside atmosphere. Atmos. Environ. 37 (29), 4109–4119.

De la Fuente, D., Vega, J.M., Viejo, F., Díaz, I., Morcillo, M., 2013. Mapping air pollution effects on atmospheric degradation of cultural heritage. J. Cult. Herit. 14, 138–145.

Drinovec, L., Mocnik, G., Zotter, P., Prévôt, A. S. H., Ruckstuhl, C., Coz, E., Rupakheti, M., Sciare, J., Müller, T., Wiedensohler, A., Hansen, A. D. A., 2015. The “dual-spot” Aethalometer: an improved measurement of aerosol black carbon with real-time loading compensation. Atmos. Meas. Tech. 8 (5), 1965–1979. http://dx.doi.org/10.5194/amt-8-1965-2015.

Ealo, M., Alastuey, A., Ripoll, A., Pérez, N., Minguillón, M.C., Querol, X., Pandolfi, M., 2016. Detection of Saharan dust and biomass burning events using near real-time intensive aerosol optical properties in the northwestern Mediterranean. Atmos. Chem. Phys. 16, 12567 –12586. http://dx.doi.org/10.5194/acp-16-12567-2016.

EEA, 2016. Air Quality in Europe - 2016 Report (EEA Report No. 28/2016), Copenhagen. http://www.eea.europa.eu/publications/air-quality-in-europe-2016 (last accessed April 2017).

Favez, O., Haddad, I. E., Piot, C., Boréave, A., Abidi, E., Marchand, N., Jaffrezo, J. L., Besombes, J. L., Personnaz, M. B., Sciare, J., Wortham, H., George, C., D'Anna, B., 2010. Inter-comparison of source apportionment models for the estimation of wood burning aerosols during wintertime in an Alpine city (Grenoble, France). Atmos. Chem. Phys. 10, 5295–5314, http://dx.doi.org/10.5194/acp-10-5295-2010.

Fort, R., 2007. La contaminación atmosférica en el deterioro del patrimonio monumental: Medidas de prevención. Ciencia, Tecnología y Sociedad para una conservación sostenible del patrimonio pétreo. Dpto. Publicaciones Universidad Popular José Hierro, San Sebastián de los Reyes, 57–70.

Ghedini, N., Ozga, I., Bonazza, A., Dilillo, M., Cachier, H., Sabbioni, C., 2011. Atmospheric aerosol monitoring as a strategy for the preventive conservation of urban monumental heritage: The Florence Baptistery. Atmos. Environ. 45, 5979–5987.

Granados-Muñoz, M. J., Navas-Guzmán, F., Bravo-Aranda, J. A., Guerrero-Rascado, J. L., Lyamani, H., Fernández-Gálvez, J., Alados-Arboledas, L., 2012. Automatic determination of the planetary boundary layer height using lidar: one-year analysis over southeastern Spain. J. Geophys. Res. 117, D18208. http://dx.doi.org/10.1029/2012JD017524

Graue, B., Siegesmund, S., Oyhantcabal, P., Naumann, R., Licha, T., Simon, K., 2013. The effect of air pollution on stone decay: the decay of the Drachenfels trachyte in industrial, urban, and rural environments—a case study of the Cologne, Altenberg and Xanten cathedrals. Environ. Earth Sci. 69 (4), 1095–1124. http://dx.doi.org/10.1007/s12665-012-2161-6.

Grossi, C.M., Brimblecombe, P., 2004. Aesthetics and perception of soiling. In: Saiz-Jimenez C. (ed.) Air pollution and cultural heritage. A. A. Balkema, Rotterdam, 199–208.

Guerreiro, C.B., Foltescu, V., de Leeuw, F., 2014. Air quality status and trends in Europe. Atmos. Environ. 98, 376–384. http://dx.doi.org/10.1016/j.atmosenv.2014.09.017.

Hamilton, R.S., Mansfield, T.A., 1991. Airborne particulate elemental carbon: its sources, transport and contribution to dark smoke and soiling. Atmos. Environ. 25, 715–723.

Hansen, A. D. A., Rosen, H., and Novakov, T., 1984. The aethalometer –an instrument for the real-time measurement of optical absorption by aerosol particles, Sci. Total Environ. 36, 191–196.

Herich, H., Hueglin, C., Buchmann, B., 2011. A 2.5 year's source apportionment study of black carbon from wood burning and fossil fuel combustion at urban and rural sites in Switzerland. Atmos. Meas. Tech. 4, 1409–1420. http://dx.doi.org/10.5194/amt-4-1409-2011.

Horemans, B., Cardell, C., Bencs, L., Kontozova-Deutsch, V., De Wael, K., Van Grieken, R., 2011. Evaluation of airborne particles at the Alhambra monument in Granada, Spain. Microchem. J. 99, 429–438. http://dx.doi.org/10.1016/j.microc.2011.06.018.

Horton, D. E., Skinner, C. B., Singh, D., Diffenbaugh, N.S., 2014. Occurrence and persistence of future atmospheric stagnation events. Nature Clim. Change, 4, 698–703.

IPCC, 2013. Climate change 2013: the physical science basis. In: Stocker, T.F., Qing, D., Plattner, G.-K., Tignor, M., Allen, S. K., Boschung, J., Nauels, A., Xia, Y., Bex, V. & Midgley, P.M. (eds.) Contribution of Working Group 1 to the Fifth Assessment Report of the Intergovernmental Panel on Climate change. Cambridge University Press, Cambridge, UK, 1535 pp.

Ivaskova, M., Kotes, P., Bradman, M., 2015. Air Pollution as important factor in construction materials deterioration in Slovak Republic. Procedia Eng. 108, 131–138.

Kirchstetter, T.W., Novakov, T., Hobbs, P.V., 2004. Evidence that the spectral dependence of light absorption by aerosols is affected by organic carbon. J. Geophys. Res. 109, D21208. http://dx.doi.org/10.1029/2004JD004999.

Kontozova-Deutsch, V., Cardell, C., Urosevic, M., Ruiz-Agudo, E., Deutsch, F., Van Grieken, R., 2011. Characterization of indoor and outdoor atmospheric pollutants impacting architectural monuments: the case of San Jerónimo Monastery (Granada, Spain). Environ. Earth Sci., 63, 1433–1445.

Krupińska, B., Van Grieken, R., De Wael, K., 2013. Air quality monitoring in a museum for preventive conservation: results of a three-year study in the Plantin-Moretus Museum in Antwerp, Belgium. Microchem. J. 110, 350–360. http://dx.doi.org/10.1016/j.microc.2013.05.006.

Lyamani, H., Olmo, F.J., Alados-Arboledas, L., 2005. Saharan dust outbreak over southeastern Spain as detected by sun photometer. Atmos. Environ. 39, 7276–7284.

Lyamani, H., Olmo, F.J., Alados-Arboledas, L., 2008. Light scattering and absorption properties of aerosol particles in the urban environment of Granada. Spain. Atmos. Environ. 42, 2630–2642.

Lyamani, H., Olmo, F.J., Alados-Arboledas, L., 2010. Physical and optical properties of aerosols over an urban location in Spain: seasonal and diurnal variability. Atmos. Chem. Phys. 10, 239–254.

Lyamani, H., Olmo, F.J., Foyo, I., Alados-Arboledas, L., 2011. Black carbon aerosols over an urban area in south-eastern Spain: changes detected after the 2008 economic crisis. Atmos. Environ. 45, 6423 –6432.

Lyamani, H., Fernández-Gálvez, J., Pérez-Ramírez, D., Valenzuela, A., Antón, M., Alados, I., Titos, G., Olmo, F. J., Alados-Arboledas, L,. 2012. Aerosol properties over two urban sites in South Spain during an extended stagnation episode in winter season. Atmos. Environ. 62, 424–432.

Meunier, V., Löhnert, U., Kollias, P., Crewell, S., 2013. Biases caused by the instrument bandwidth and beam width on simulated brightness temperature measurements from scanning microwave radiometers. Atmos. Meas. Tech., 6, 1171–1187. http://dx.doi.org/10.5194/amt-6-1171-2013.

Milford, C., Fernández-Camacho, R., de la Campa, A. S., Rodríguez, S., Castell, N., Marrero, C., Bustos, J. J., de la Rosa, J. D., Stein, A. F., 2016. Black Carbon aerosol measurements and simulation in two cities in south-west Spain. Atmos. Environ. 126, 55–65. http://dx.doi.org/10.1016/j.atmosenv.2015.11.026.

Minguillón, M. C., Ripoll, A., Pérez, N., Prévôt, A. S. H., Canonaco, F., Querol, X., Alastuey, A., 2015. Chemical characterization of submicron regional background aerosols in the western Mediterranean using an Aerosol Chemical Speciation Monitor. Atmos. Chem. Phys. 15, 6379–6391. http://dx.doi.org/10.5194/acp-15-6379-2015.

Moosmüller, H., Chakrabarty, R.K., Arnott, W.P., 2009. Aerosol light absorption and its measurement: a review. J. Quant. Spectrosc. Rad. Trans. 110, 844–878.

Nava, S., Becherini, F., Bernardi, A., Bonazza, A., Chiari, M., García-Orellana, I., Lucarelli, F., Ludwig, N., Migliori, A., Sabbioni, C., Udisti, R., Valli, G., Vecchi R., 2010. An integrated approach to assess air pollution threats to cultural heritage in a semi-confined environment: The case study of Michelozzo's Courtyard in Florence (Italy). Sci. Total Environ. 408, 1403–1413.

Navas-Guzmán, F., Guerrero-Rascado, J. L., Fernández-Medina, A. B., Adame, J. A., Alados-Arboledas, L., 2007. Mixing layer height determination by Lidar and radiosounding data. European Aerosol Conference 2007, Salzburg, Austria, 9–14 September 2007, Cd1, T20A014.

Navas-Guzmán, F., Fernández-Gálvez, J., Granados-Muñoz, M. J., Guerrero-Rascado, J. L., Bravo-Aranda, J. A., Alados-Arboledas, L. 2014. Tropospheric water vapour and relative humidity profiles from lidar and microwave radiometry. Atmos. Meas. Tech. 7 (5), 1201–1211. http://dx.doi.org/10.5194/amt-7-1201-2014.

Pappalardo, G., Amodeo, A., Apituley, A., Comeron, A., Freudenthaler, V., Linné, H., Ansmann, A., Bösenberg, J., D'Amico, G., Mattis, I., Mona, L., Wandinger, U., Amiridis, V., Alados-Arboledas, L., Nicolae, D., Wiegner, M., 2014. EARLINET: Towards an advanced sustainable European aerosol lidar network. Atmos. Meas. Tech. 7 (8), 2389–2409.

Querol, X., Alastuey, A., Viana, M., Moreno, T., Reche, C., Minguillón, M.C., Ripoll, A., Pandolfi, M., Amato, F., Karanasiou, A., Pérez, N., Pey, J., Cusack, M., Vázquez, R., Plana, F., Dall’Osto, M., de la Rosa, J., Sánchez de la Campa, A., Fernández-Camacho, R., Rodríguez, S., Pio, C., Alados-Arboledas, L., Titos, G., Artíñano, B., Salvador, P., García Dos Santos, S., Fernández Patier, R., 2013. Variability of carbonaceous aerosols in remote, rural, urban and industrial environments in Spain: Implications for air quality policy. Atmos. Chem. Phys. 13 (13), 6185–6206.

Pereira, S.N., Wagner F., and Silva A.M,. 2012. Long term black carbon measurements in the southwestern Iberia Peninsula. Atmos. Environ. 57, 63-71.

Reche, C., Querol, X., Alastuey, A., Viana, M., Pey, J., Moreno, T., Rodríguez, S., González, Y., Fernández-Camacho, R., de la Rosa, J., Dall'Osto, M., Prévôt, A. S. H., Hueglin, C., Harrison, R. M., Quincey, P., 2011. New considerations for PM, Black Carbon and particle number concentration for air quality monitoring across different European cities. Atmos. Chem. Phys. 11, 6207–6227. http://dx.doi.org/10.5194/acp-11-6207-2011.

Rodriguez-Navarro, C., Sebastian, E., 1996. Role of particulate matter from vehicle exhaust on porous building stones (limestone) sulfation. Sci. Total Environ. 187, 79–91.

Rolph, G.D., 2017. Real-time Environmental Applications and Display sYstem (READY) Website (http://www.ready.noaa.gov). NOAA Air Resources Laboratory, College Park, MD.

Rose, T., Crewell, S., Löhnert, U., Simmer, C., 2005. A network suitable microwave radiometer for operational monitoring of the cloudy atmosphere. Atmos. Res., 75, 183–200, http://dx.doi.org/10.1016/j.atmosres.2004.12.005.

Sabbioni, C., Ghedini, N., Bonazza, A., 2003. Organic anions in damage layers on monuments and buildings. Atmos. Environ. 37 (9), 1261–1269.

Saha, A., Despiau, S., 2009. Seasonal and diurnal variations of black carbon aerosols over a Mediterranean coastal zone. Atmos. Res. 92, 27-41.

Sandradewi, J., Prévôt, A.S.H., Szidat, S., Perron, N., Alfarra, M.R., Lanz, V.A., Weingartner, E., Baltensperger, U., 2008. Using aerosol light absorption measurements for the quantitative determination of wood burning and traffic emission contributions to particulate matter. Environ. Sci. Technol. 42 (9), 3316–3323. http://dx.doi.org/10.1021/es702253m.

Segura, S., Estellés, V., Titos, G., Lyamani, H., Utrillas, M.P., Zotter, P., Prévôt, A.S.H., Mocnik, G., Alados-Arboledas, L., Martínez-Lozano, J.A., 2014. Determination and analysis of in situ spectral aerosol optical properties by a multiinstrumental approach. Atmos. Meas. Tech. 7, 2373–2387. http://dx.doi.org/10.5194/amt-7-2373-2014

Stein, A.F., Draxler, R.R, Rolph, G.D., Stunder, B.J.B., Cohen, M.D., and Ngan, F., 2015. NOAA's HYSPLIT atmospheric transport and dispersion modeling system. Bull. Amer. Meteor. Soc., 96, 2059-2077. http://dx.doi.org/10.1175/BAMS-D-14-00110.1.

Titos, G., Lyamani, H., Pandolfi, M., Alastuey, A., Alados-Arboledas, L., 2014. Identification of fine (PM_1) and coarse (PM_{10-1}) sources of particulate matter in an urban environment. Atmos. Environ. 89, 593-602.

Titos, G., Lyamani, H., Drinovec, L., Olmo, F. J., Močnik, G., Alados-Arboledas, L., 2015. Evaluation of the impact of transportation changes on air quality. Atmos. Environ. 114, 19-31.

Titos, G., Del Águila, A., Cazorla, A., Lyamani, H., Casquero-Vera, J.A., Colombi, C., Cuccia, E., Gianelle, V., Močnik, G., Alastuey, A., Olmo, F.J., Alados-Arboledas, L., 2017. Spatial and temporal variability of carbonaceous aerosols: Assessing the impact of biomass burning in the urban environment. Sci. Total Environ. 578, 613-625.

Tiwari, S., Srivastava, A.K., Bisht, D.S., Parmita, P., Srivastava, M.K., Attri, S.D., 2013. Diurnal and seasonal variations of black carbon and $PM_{2.5}$ over New Delhi, India: influence of meteorology. Atmos. Res. 125-126. http://dx.doi.org/10.1016/j.atmosres.2013.01.011.

Uria-Tellaetxe, I., Carslaw, D.C., 2014. Conditional bivariate probability function for source identification. Environ. Model. Softw. 59, 1–9.

Urosevic, M., Yebra-Rodríguez, A., Sebastián-Pardo, E., Cardell, C., 2012. Black soiling of an architectural limestone during two-year term exposure to urban air in the city of Granada (S Spain). Sci. Total Environ. 414, 564-575.

Valenzuela, A., Olmo, F.J., Lyamani, H., Antón, M., Titos, G., Cazorla, A., Alados-Arboledas, L., 2015. Aerosol scattering and absorption Angström exponents as indicators of dust and dust-free days over Granada (Spain). Atmos. Res. 154, 1–13.

Vestreng, V., Myhre, G., Fagerli, H., Reis, S., and Tarrasón, L., 2007. Twenty-five years of continuous sulphur dioxide emission reduction in Europe, Atmos. Chem. Phys. 7, 3663–3681.

Viana, M., Maenhaut, W., Ten Brink, H. M., Chi, X., Weijers, E., Querol, X., Alastuey, A., Mikuskae, P., Vecera, Z., 2007. Comparative analysis of organic and elemental carbon concentrations in carbonaceous aerosols in three European cities. Atmos. Environ. 41 (28), 5972–5983. http://dx.doi.org/10.1016/j.atmosenv.2007.03.035.

Virkkula, A., Măkelă, T., Hillamo, R., Yli-Tuomi, T., Hirsikko, A., Hămeri, K. and Koponen, K.I., 2007. A simple procedure for correcting loading effects of aethalometer data. J. Air Waste Manage. Assoc. 57, 1214–1222.

Weingartner, E., Saathoff, H., Schnaiter, M., Streit, N., Bitnar, B., Baltensperger, U., 2003. Absorption of light by soot particles: determination of the absorption coefficient by means of Aethalometers. J. Aerosol Sci. 34, 1445–1463.

Whiteman, C.D., Hoch, S.W., Horel, J.D., Charland, A., 2014. Relationship between particulate air pollution and meteorological variables in Utah's Salt Lake Valley. Atmos. Environ. 94, 742–753.